

Conf-931193--1

UCRL-JC-115167
PREPRINT

**Dual-Band Infrared Imaging
for
Quantitative Corrosion Detection in Aging Aircraft**

N. K. Del Grande

RECEIVED
DEC 17 1993
OSTI

**This paper was prepared for submittal to the
ASNT (American Society for Nondestructive Testing)
Fall Conference, Long Beach, California
November 9-11, 1993**

November 1993

 Lawrence
Livermore
National
Laboratory

This is a preprint of a paper intended for publication in a journal or proceedings. Since changes may be made before publication, this preprint is made available with the understanding that it will not be cited or reproduced without the permission of the author.

DISTRIBUTION OF THIS DOCUMENT IS UNLIMITED

DISCLAIMER

This document was prepared as an account of work sponsored by an agency of the United States Government. Neither the United States Government nor the University of California nor any of their employees, makes any warranty, express or implied, or assumes any legal liability or responsibility for the accuracy, completeness, or usefulness of any information, apparatus, product, or process disclosed, or represents that its use would not infringe privately owned rights. Reference herein to any specific commercial products, process, or service by trade name, trademark, manufacturer, or otherwise, does not necessarily constitute or imply its endorsement, recommendation, or favoring by the United States Government or the University of California. The views and opinions of authors expressed herein do not necessarily state or reflect those of the United States Government thereof, and shall not be used for advertising or product endorsement purposes.

DUAL-BAND INFRARED IMAGING FOR QUANTITATIVE CORROSION DETECTION IN AGING AIRCRAFT

N. K. Del Grande
Lawrence Livermore National Laboratory
P. O. Box 808, Livermore CA 94550
(510) 422-1010

ABSTRACT

Aircraft skin thickness-loss from corrosion has been measured using dual-band infrared (DBIR) imaging on a flash-heated Boeing 737 fuselage structure. We mapped surface temperature differences of 0.2 to 0.6 °C for 5 to 14 % thickness losses within corroded lap splices at 0.4 seconds after the heat flash. Our procedure mapped surface temperature differences at sites without surface-emissivity clutter (from dirt, dents, tape, markings, ink, sealants, uneven paint, paint stripper, exposed metal and roughness variations). We established the correlation of percent thickness loss with surface temperature rise using a partially corroded F-18 wing box and several aluminum panels which had thickness losses from milled flat-bottom holes. We mapped the lap splice composite thermal inertia, $(kpc)^{1/2}$, which characterized shallow skin defects within the lap splice at early times (<0.3 s) and deeper skin defects within the lap splice at late times (>0.4 s). Corrosion invaded the inside of the Boeing 737 lap splice, beneath the galley and the latrine, where we observed "pillowing" from volume build-up of corrosion by-products.

1.0 EMISSIVITY CORRECTED TEMPERATURE MAPS

Using DBIR image ratios (from DBIR cameras which scan infrared at 3-5 μm and 8-12 μm) we were able to enhance surface temperature contrast and remove the mask of surface emissivity clutter (from dirt, dents, tape, markings, ink, sealants, uneven paint, paint stripper, exposed metal and roughness variations). This clarified interpretation of subtle heat flow anomalies associated with hidden defects and corrosion. We computed the following DBIR image ratios of enhanced temperature contrast (T^5) and emissivity-ratio (E-ratio) maps:

$$(T/T_{av})^5 = (S/S_{av}) / (L/L_{av}) \quad (1)$$

$$\text{E-ratio} = (L/L_{av})^2 / (S/S_{av}) \quad (2)$$

where S is the short-wavelength intensity (e.g., I_5), S_{av} is the average value of the pixels in S , L is the long wavelength intensity (e.g., I_{10}) and L_{av} is the average value of the pixels in L . See Figure 1 for the Boeing 737 images of the above temperature and emissivity-ratio maps which allowed us to distinguish corrosion-related thickness loss effects and surface emissivity clutter (from dirt, dents, tape, markings, ink, sealants, uneven paint, paint stripper, exposed metal and roughness variations).

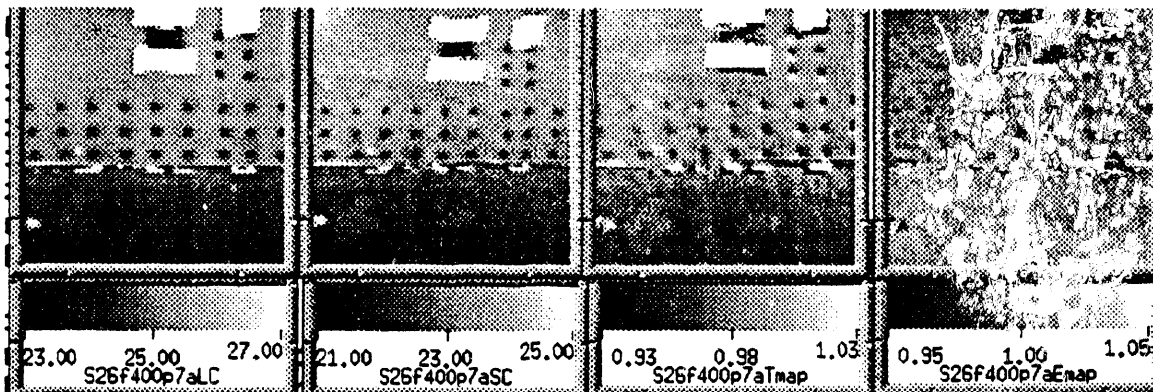


Figure 1. Maps (left to right) of Boeing 737 lap splice structure with hidden defects showing 10 μm and 5 μm apparent temperatures ($^{\circ}\text{C}$), dual-band infrared (DBIR) enhanced temperatures (relative scale) and emissivity differences from clutter.

MASTER
DISTRIBUTION OF THIS DOCUMENT IS UNLIMITED

YJ

2.0 DYNAMIC TEMPERATURE CHANGES FOR FLASH-HEATED LAP SPLICE

Corrosion within the Boeing 737 (epoxy-bonded) lap splice causes disbonding. Trapped by-products act as an insulator, delaying heat transfer by conduction from the front to the back surface. This effect is shown in Figure 2 by the near-constant temperature contrast from 0.4 to 3.2 s which is based on our measurements of the FAA owned Boeing 737 which was inspected at the Aging Aircraft NDI Center (AANC), at a Sandia hangar in Albuquerque, New Mexico.

Corrosion-related material loss effects are best measured at 0.4 seconds after the heat flash. Temperatures at 0.4 s are sensitive to material loss effects within a lap splice and insensitive to timing uncertainties. The timing is early enough to provide a good temperature contrast for sites with and without material loss from corrosion. At later times, trapped materials mask the temperature-time history which characterizes material-loss effects for corrosion sites.

We established the correlation between percent thickness loss and above-ambient surface temperature rise, at 0.4 seconds after the heat flash, based on our measurements for five specimens which averaged a $24 \pm 5\%$ thickness loss per $^{\circ}\text{C}$ temperature rise. These specimens included a F-18 partially corroded wing box (with a 2.9 mm uncorroded thickness) and four 1.0 mm to 3.9 mm thickness aluminum panels with milled flat-bottom holes which had thickness losses ranging from 6% to 62%.

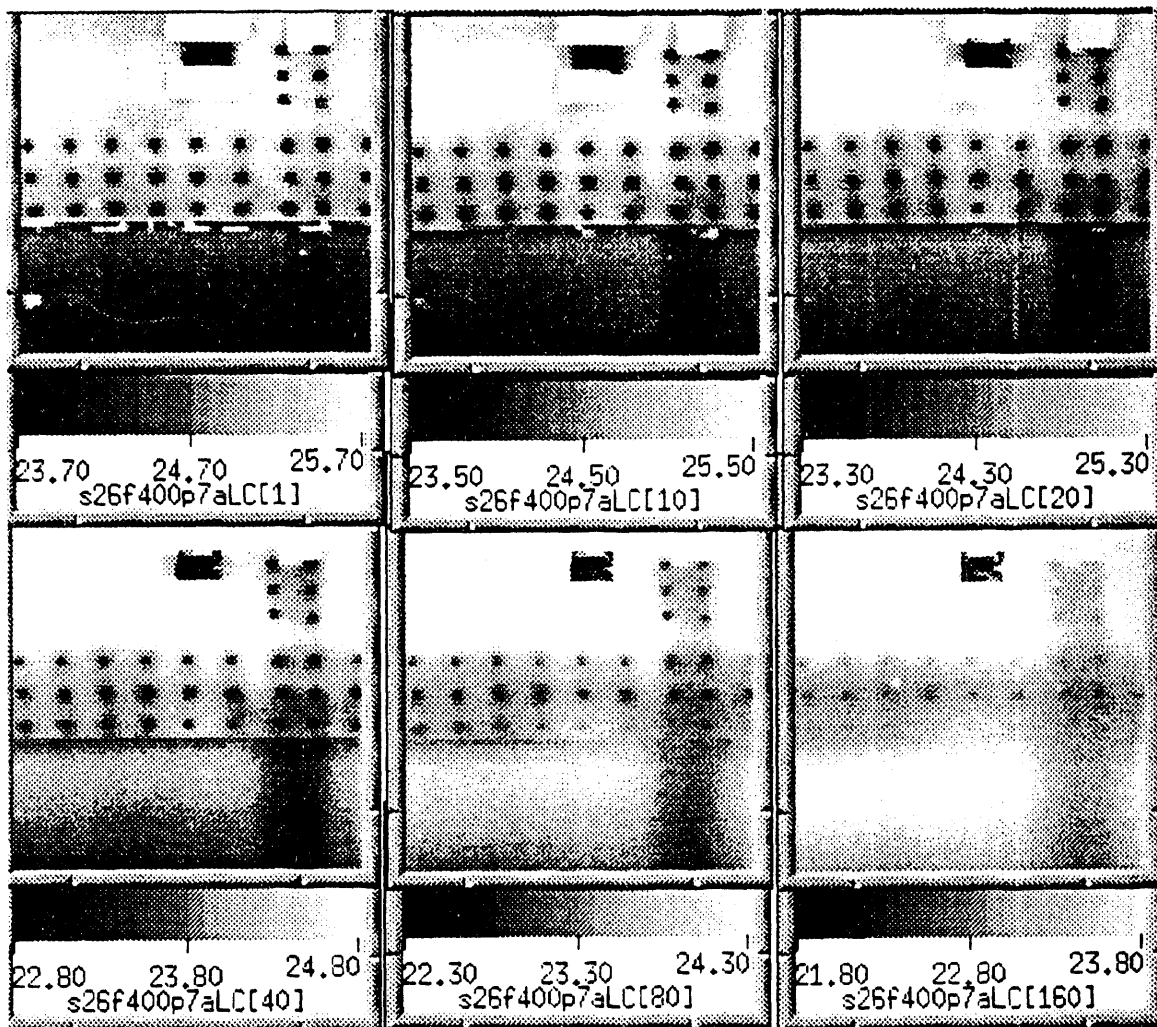


Figure 2. The dynamic temperature variations for the Boeing 737 lap splice images at 0.04 s, 0.4 s and 0.8 s (top left to right) and at 1.6 s, 3.2 s and 6.4 s (bottom left to right) based on the 10 μm apparent temperature maps.

3.0 THERMAL INERTIA MAPPING

A solution to the heat transfer equation for a thick panel with an instantaneous surface heat flux is:

$$T(x, t) = \frac{q}{\sqrt{4\pi k\rho c t}} \exp\left(-\frac{x^2}{4\alpha t}\right) \quad (3)$$

where T is temperature, x is the distance from the surface, k is thermal conductivity, ρ is density, c is heat capacity, α is thermal diffusivity, t is time and q is the surface heat flux. For a semi-infinite solid approximation, the surface temperature is proportional to the inverse square root of time. In practice, we map the fuselage composite thermal inertia, $(kpc)^{1/2}$, based on the (inverse) slope of the surface temperature versus inverse square root of time. Composite thermal inertia maps characterize shallow skin defects within the lap splice at early times (<0.3 s) and deeper skin defects within the lap splice at late times (>0.4 s). Late time composite thermal inertia maps depict where corrosion-related thickness losses occur.

We note in Figure 3 (right side) a butterfly-like pattern at the upper right side. This is where the corrosive activity invaded the inside (upper lap edge) of the Boeing 737 lap splice on Stringer 26, near station F400.7, beneath the galley and the latrine. Typical visible signs of corrosion were also evident (e.g., pillowing) resulting from the increased volume of corrosion by-products within the lap splice, between the rivet heads.

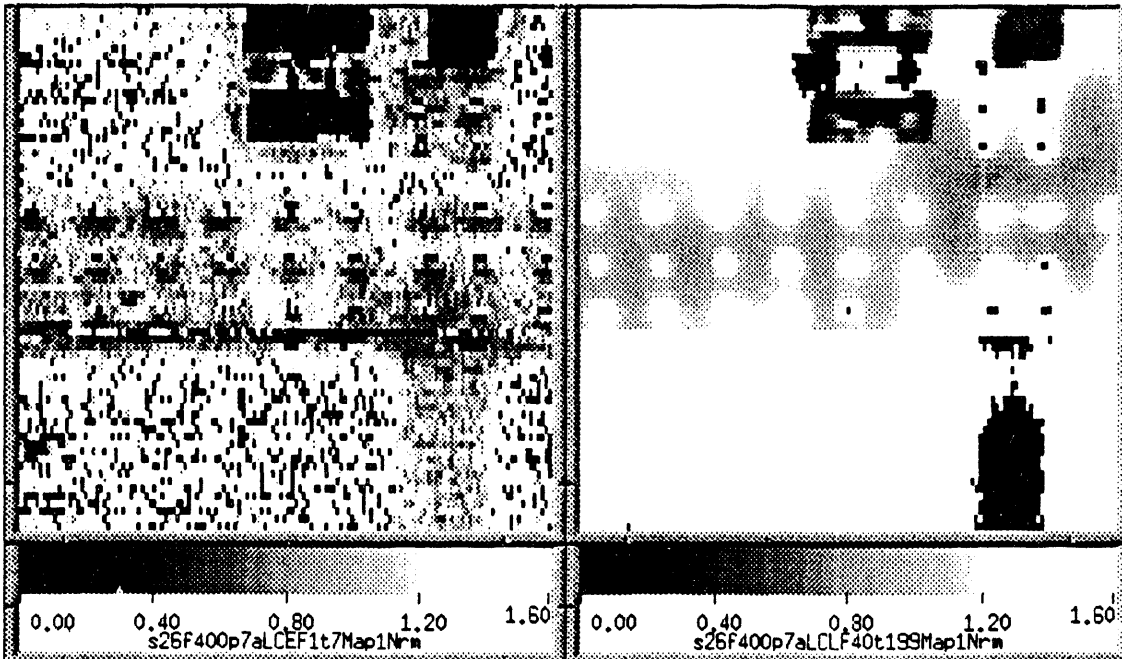
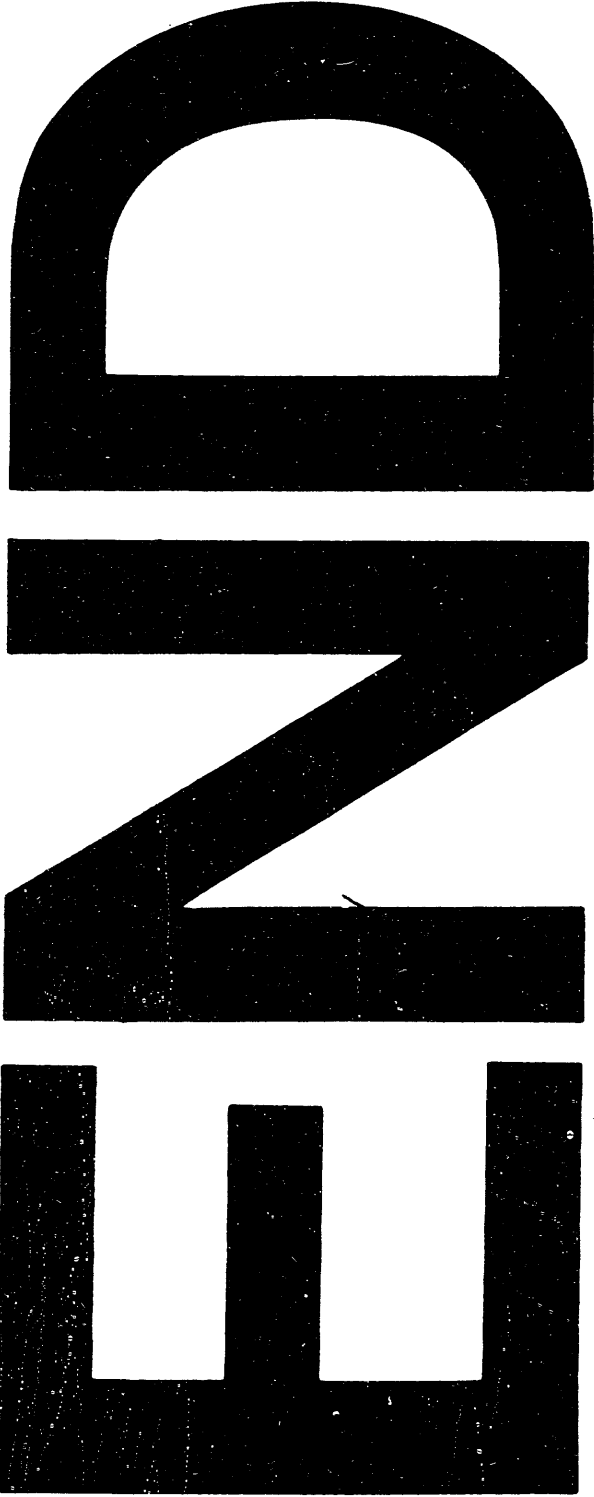


Figure 3. Seven early-time (less than 0.28 s, on the left) and 159 late-time (1.6 s to 8.0 s, on the right) images were used to produce composite thermal inertia maps of the Boeing 737 aircraft fuselage lap splice shown above. Note the relatively low thermal inertia for the front-surface cloth tape and masking tape markers (top center and right corner) and the back surface tear strap (bottom right corner).

4.0 ACKNOWLEDGMENTS

This work was performed by LLNL under the auspices of DOE contract number W-7405-ENG-48 for the FAA Aging Aircraft Non-Destructive Inspection R&D Program, Interagency Agreement DTFA03-92-A-00007. We thank Chris Seher, P. K. Bhagat and David Galella at the FAA Technical Center for their helpful suggestions. We are grateful for the support efforts of Gary Phipps, Craig Jones, Don Harmon and Pat Walter at Sandia National Laboratory, Albuquerque, NM and Dr. Satish Kulkarni, NDE Section Leader at LLNL. Also, we acknowledge the collaboration of Ken Dolan, Project Leader, Phil Durbin, DBIR technology specialist and Michael Gorvad, signal processing engineer for their participation on the FAA Aging Aircraft NDI demonstration of the DBIR imaging technique conducted on the aged Boeing 737 aircraft at the FAA/AANC hangar.



DATA
TELEGRAM
TO
QUICK
SIGHT

